Carbohydrate Polymers 98 (2013) 139–145

Contents lists available at SciVerse ScienceDirect

Carbohydrate Polymers

journal homepage: www.elsevier.com/locate/carbpol

Properties of polylactic acid composites reinforced with oil palm biomass microcrystalline cellulose

M.K. Mohamad Haafiz[a,b], Azman Hassan[a,*], Zainoha Zakaria[c], I.M. Inuwa[a], M.S. Islam[d], M. Jawaid[e]

[a] Department of Polymer Engineering, Faculty of Chemical, Universiti Teknologi Malaysia, UTM 81310 Skudai, Johor, Malaysia
[b] School of Industrial Technology, Universiti Sains Malaysia, 11800 Penang, Malaysia
[c] Faculty of Science, Universiti Teknologi Malaysia, UTM 81310 Skudai, Johor, Malaysia
[d] Department of Chemistry, Faculty of Science, Universiti Putra Malaysia, Serdang, Selangor, Malaysia
[e] Biocomposite Laboratory, Institute of Tropical Forestry and Forest Products, Universiti Putra Malaysia, Serdang, Selangor, Malaysia

ARTICLE INFO

Article history:
Received 26 March 2013
Received in revised form 29 April 2013
Accepted 24 May 2013
Available online 2 June 2013

Keyword:
Microcrystalline cellulose
Thermal properties
Atomic force microscopy
Casting

ABSTRACT

In this work, polylactic acid (PLA) composites filled with microcrystalline cellulose (MCC) from oil palm biomass were successfully prepared through solution casting. Fourier transform infrared (FT-IR) spectroscopy indicates that there are no significant changes in the peak positions, suggesting that incorporation of MCC in PLA did not result in any significant change in chemical structure of PLA. Thermogravimetric analysis was conducted on the samples. The T_{50} decomposition temperature improved with addition of MCC, showing increase in thermal stability of the composites. The synthesized composites were characterized in terms of tensile properties. The Young's modulus increased by about 30%, while the tensile strength and elongation at break for composites decreased with addition of MCC. Scanning electron microscopy (SEM) of the composites fractured surface shows that the MCC remained as aggregates of crystalline cellulose. Atomic force microscopy (AFM) topographic image of the composite surfaces show clustering of MCC with uneven distribution.

1. Introduction

Nowadays, production of sustainable and environmental friendly sources of energy also known as green materials has generated enormous attention and interest in both academic and industrial fields. This interest arose due to the growing concern for environmental protection and the rising cost of fossil fuel worldwide (Bondeson, Mathew, & Oksman, 2006; Maria, Garcia, & Lagaron, 2010; Oksman, Mathew, Bondeson, & Kvien, 2006; Suryanegara, Nakagaito, & Yano, 2009). One of the approaches taken recently to curb the problems is through application of biopolymers which are naturally occurring polymers found in all living organisms (Petersson, Kvien, & Oksman, 2007). The use of biopolymers as a source of raw material for plastics production will provide huge advantages in terms of environmental conservation efforts when compared to the use of fossil fuel due to its less harmful effect (Bondeson, Mathew, & Oksman, 2006; Oksman, Mathew, Bondeson, & Kvien, 2006; Petersson, Kvien, & Oksman, 2007; Suryanegara, Nakagaito, & Yano, 2009). Biopolymers can be obtained from agricultural feedstock, marine fauna, and microbial activities (Maria, Garcia, & Lagaron, 2010; Oksman, Mathew, Bondeson, & Kvien, 2006; Petersson, Kvien, & Oksman, 2007; Suryanegara, Nakagaito, & Yano, 2009). Recently researchers reported the use of biopolymers as a potential polymer matrix for the synthesis of biodegradable and environmentally friendly composites such as soy–oil based epoxy, starch based polymers, polycaprolactone (PCL), polyhydroxy butyrate (PHB), polyester amide and polylactic acid (PLA) (Mathew, Oksman, & Sain, 2005).

PLA is bio-degradable thermoplastic aliphatic polyester which can be derived from renewable resources such as starch (Jonoobi, Harun, Mathew, & Oksman, 2010; Nakagaito, Fujimura, Sakai, Hama, & Yano, 2009; Petersson & Oksman, 2006). It has been used in several applications such as food packaging, water and milk bottles, barriers for sanitary products and diapers, as well as in automotive applications (Jonoobi, Harun, Mathew, & Oksman, 2010; Maria, Garcia, & Lagaron, 2010; Nakagaito, Fujimura, Sakai, Hama, & Yano, 2009; Petersson, Kvien, & Oksman, 2007). However, low thermal stability, low water vapour and gas barrier properties as well as embrittlement have limited its use in certain applications such as high temperature environment

* Corresponding author at: Department of Polymer Engineering, Faculty of Chemical and Natural Resources Engineering, Universiti Teknologi Malaysia, 81300 Skudai, Johor, Malaysia. Tel.: +60 7 5537835; fax: +60 7 5581 463.
E-mail addresses: azmanh@cheme.utm.my, AZMANH@CHEME.UTM.MY (A. Hassan).

0144-8617/$ – see front matter © 2013 Elsevier Ltd. All rights reserved.
http://dx.doi.org/10.1016/j.carbpol.2013.05.069

(Maria, Garcia, & Lagaron, 2010; Oksman, Mathew, Bondeson, & Kvien, 2006; Petersson & Oksman, 2006; Qu, Goa, Wu, & Zhang, 2010). In order to overcome these inherent shortcomings reinforcing fillers are now incorporated to improve these properties while maintaining their inherently good properties such as transparency and biodegradability (Maria, Garcia, & Lagaron, 2010; Mathew, Oksman, & Sain, 2005; Petersson & Oksman, 2006).

The used of nanoclays as reinforcement for polymeric materials have been extensively studied (Maria, Garcia, & Lagaron, 2010; Oksman, Mathew, Bondeson, & Kvien, 2006). In order to produce a fully degradable and renewable nanocomposite, substituting the clay with cellulose based reinforcement is the best alternative (Oksman, Mathew, Bondeson, & Kvien, 2006). Cellulose is one of the abundant materials in nature. It is a renewable and biodegradable material, cheaply sourced, widely available, low-energy consumption and has good mechanical properties such as high modulus (~140 GPa; Sturcova, Davies, & Eichhorn (2005)), as compared to other inorganic reinforcing fillers. Another advantage of cellulose is its fibrous nature which can align and orient along matrix axis improving mechanical properties with less weight compared to clay based fillers. It also has high sound attenuation and comparatively easy processability due to its nonabrasive nature, allows high filling levels which in turn results in significant cost savings (Eichhorn et al., 2010; Pullawan, Wilkinson, & Eichhorn, 2010; Samir, Alloin, & Dufresne, 2005).

Cellulose consists of crystalline and amorphous phase at nanometer range (Qu, Goa, Wu, & Zhang, 2010). The latter is readily hydrolysed when subjected to strong acid hydrolysis and mechanical force. Acid hydrolysis is able to remove amorphous region as well as reduces the degree of polymerization of the cellulose chain with almost no weight loss (Rånby, 1951). These hydrolysed materials are referred to as microcrystal or microcrystalline cellulose (MCC) (Battista, 1950; Kumar, Maria De La, & Yang, 2002; Siqueira, Bras, & Dufresne, 2009). MCC is well known as a biodegradable material, which is used for packaging food products and widely used in different industrial fields, such as pharmaceuticals, cosmetics, medical applications and food processing (Kumar, Maria De La, & Yang, 2002; Petersson & Oksman, 2006; Zhou, Yu, Zhu, & Qin, 2011).

At present MCC is commercially available in different grades and can be obtained on an industrial scale through hydrolysis of wood and cotton using dilute mineral acids (El-Sakhawy & Hassan, 2007). MCC is characterized by a high degree of crystallinity, and the values typically in the range between 55 and 80% as determined by X-ray diffraction. The characteristic features of MCC depends on the origin of the cellulosic sources and processing variables, such as reaction temperature and duration, mechanical agitation of the slurry, and drying conditions (Chuayjuljit, Su-uthai, & Charuchinda, 2010). The used of MCC as novel green filler in polymer matrices using polypropylene, poly (ethylene terephthalate)-poly (trimethylene terephthalate) blends to develop environmental friendly composites have been reported (Zhou, Yu, Zhu, & Qin, 2011). Chuayjuljit, Su-uthai, and Charuchinda (2010) shows increase in tensile strength and Young's modulus when MCC used as reinforcement in poly (vinyl chloride). Mathew and co-workers reported the use of MCC as filler in PLA using twin-screw extrusion process. The results showed lower mechanical properties as compare to pure PLA. However the dynamic mechanical thermal analysis (DMTA) showed that the storage modulus was increased with the addition of MCC (Mathew, Oksman, & Sain, 2005).

To the best of our knowledge, there is no single report have been made in open literature on the use of the MCC from oil palm empty fruit bunch (OPEFB) residues as reinforcement filler in PLA. The objective of this study is to evaluate the effect of MCC loading on morphological, thermal and mechanical properties of resulting PLA composites.

2. Experimental

2.1. Materials

Polylactic (NatureWork™ PLA 300ID) in pellet form was obtained from NatureWork® LLC, Minnetonka, MN USA. It has a specific gravity 1.24 g/cm^3 and melt flow index (MFI) around 15 g/10 min (190 °C/2.16 kg). Microcrystalline cellulose (MCC) was produced from oil palm empty fruit bunch (OPEFB) chlorine free pulps as the reinforcing filler. The production of MCC was described in details on our previous paper (Haafiz, Eichhorn, Hassan, & Jawaid, 2013). The reagent used was chloroform secured from Merck, Malaysia.

2.2. Preparation of PLA and PLA/MCC composite

A 10 wt% solution of PLA pellets in chloroform was prepared by stirring the solution inside the water bath at 60 °C for 2 h until the pellets were fully dissolved (Maria, Garcia, & Lagaron, 2010). The PLA solution was immediately cast on the clean glass plates and left for the solvent to evaporate at ambient temperature for 48 h. The thickness of the cast solution was approximately 100 μm and noted as pure PLA.

To prepare the PLA/MCC composites, 10 wt% solution of PLA was mixed with different amounts of MCC (1, 3 and 5 wt%) and the mixture was kept at 60 °C with strong agitation until the PLA pellets were fully dissolved. The suspension was then sonicated for 5 min and was immediately cast on a clean glass plate to generate composite thickness of ~100 μm after removal of the solvent. The composites were designated as PLA/MCC1, PLA/MCC3 and PLA/MCC5.

2.3. Characterization

Fourier transform infrared (FT-IR) was performed on a Perkin Elmer 1600 Infrared Spectrometer. FT-IR spectra of the samples were recorded by using Nicolet's AVATAR 360 at 32 scans with a resolution of 4 cm^{-1} and within the wave number range of 4000–370 cm^{-1}. The significant transmittance peak at a particular wave numbers was measured by using the "find peak tool" provided by Nicolet OMNIC 5.01 software.

Mechanical test was done using the Instron 4400 Universal Tester to measure the tensile strength at the point of breakage for each sample. Tensile tests were carried out at room temperature, according to the ASTM D882type V. A fixed crosshead rate of 10 mm/min was utilized in all cases and the results were taken as an average of five tests.

The morphology of samples was observed using scanning electron microscopy (SEM) and atomic force microscopy (AFM). SEM was conducted using a SEM-EDX Oxford INCA 400 model at an acceleration voltage 10 kV. The samples were sputter-coated with gold to avoid charging. AFM observation was performed using SPA-300HV atomic force microscopy with a SPI 3800 controller, the pure PLA and composite samples (0.1 mm × 0.1 mm) were analyzed directly.

The samples were characterized to determine their thermal stability using a thermogravimetric analyzer (TGA) model 2050, (TA Instruments, New Castle, DE). The specimens were scanned from 30 °C to 800 °C at the rate of 10 °C/min and analyses were performed under a nitrogen gas flow.

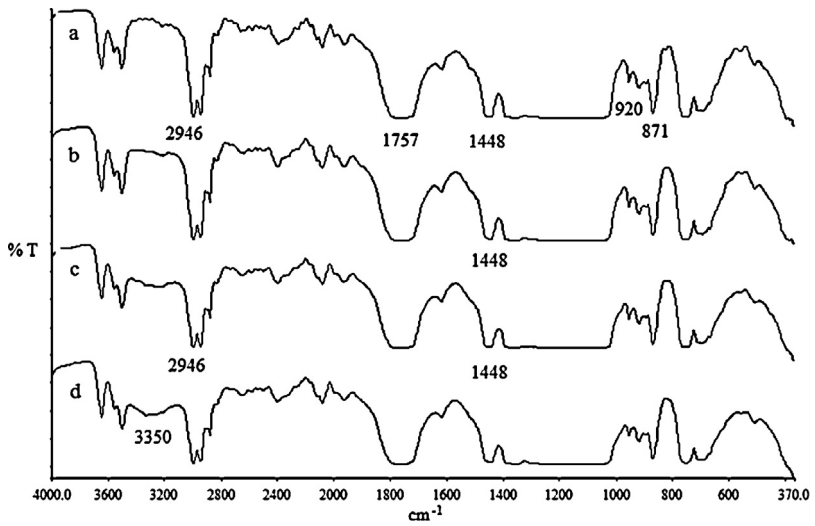

Fig. 1. Typical FT-IR spectroscopy for (a) PLA and PLA/MCC with different MCC loading ((b) 1%, (c) 3% and (d) 5%).

3. Results and discussion

3.1. FT-IR spectroscopy analysis

The FT-IR analysis has been widely used to identify the interaction and phase behavior of polymer composites (Kemala, Budianto, & Soegiyono, 2012; Qu, Goa, Wu, & Zhang, 2010). The typical FT-IR spectra of pure PLA and PLA/MCC composites are shown in Fig. 1. Fig. 1a displays the characteristic peak of pure PLA. The O—H bending and starching for PLA are apparent at 3330–3600 cm^{-1}(Kemala, Budianto, & Soegiyono, 2012; Pamula, Blazeeicz, Paluszkiewiez, & Dobrzyński, 2001). The band originated from C=O stretching vibration of carbonyl is situated at 1757 cm^{-1} (Kemala, Budianto, & Soegiyono, 2012; Pamula, Blazeeicz, Paluszkiewiez, & Dobrzyński, 2001; Qu, Goa, Wu, & Zhang, 2010). The peaks at 2946 to 2999 cm^{-1} are due to the asymmetric stretching vibration of C—H, (Kemala, Budianto, & Soegiyono, 2012; Qu, Goa, Wu, & Zhang, 2010). The peaks at 1448 cm^{-1} is attributed to the deformation of C—H in the CH_3 and the peak corresponding to C—C single bond appeared at 920 and 871 cm^{-1} (Kemala, Budianto, & Soegiyono, 2012; Qu, Goa, Wu, & Zhang, 2010).

Fig. 1(b)–(d) shows the character peak of PLA/MCC composites. The spectrum did not reveal any new peak when MCC was added. The absence of new peak suggest that the lower amount of filler used to produce the composites film only physically interacted between PLA and MCC rather than chemical interaction. This result is similar to the one reported by Qu, Goa, Wu, and Zhang (2010) when cellulose nanofibrils was used to reinforce PLA. The peak at 1757 cm^{-1} which is corresponding to C=O become broader, when the percentage of MCC added increased. According to Qu, Goa, Wu, and Zhang (2010) this was attributed to the interaction between C=O from PLA and the O—H groups from MCC. It is interesting to note that, the relatively small peaks between 3200 and 3400 cm^{-1} (O—H bond stretching deformation of PLA) disappeared in PLA/MCC composites. The peak shifted to a broad peak approximately at 3350 cm^{-1} and increased intensity as the percentage of MCC was increased. The similar finding has been reported earlier by Yew, Mohd Yusof, Mohd Ishak, and Ishiaku (2005), when PLA matrix was filled with rice starch.

3.2. Thermogravimetric analysis (TGA)

In order to investigate the thermal properties of the PLA and PLA/MCC composites, thermogravimetric analysis (TGA) were performed. Fig. 2 shows the TGA (weight% vs. temperature °C) and DTG thermograms of pure PLA and PLA/MCC composites with various MCC contents. The thermal degradation data of pure PLA and PLA/MCC are tabulated in Table 1, using the temperatures

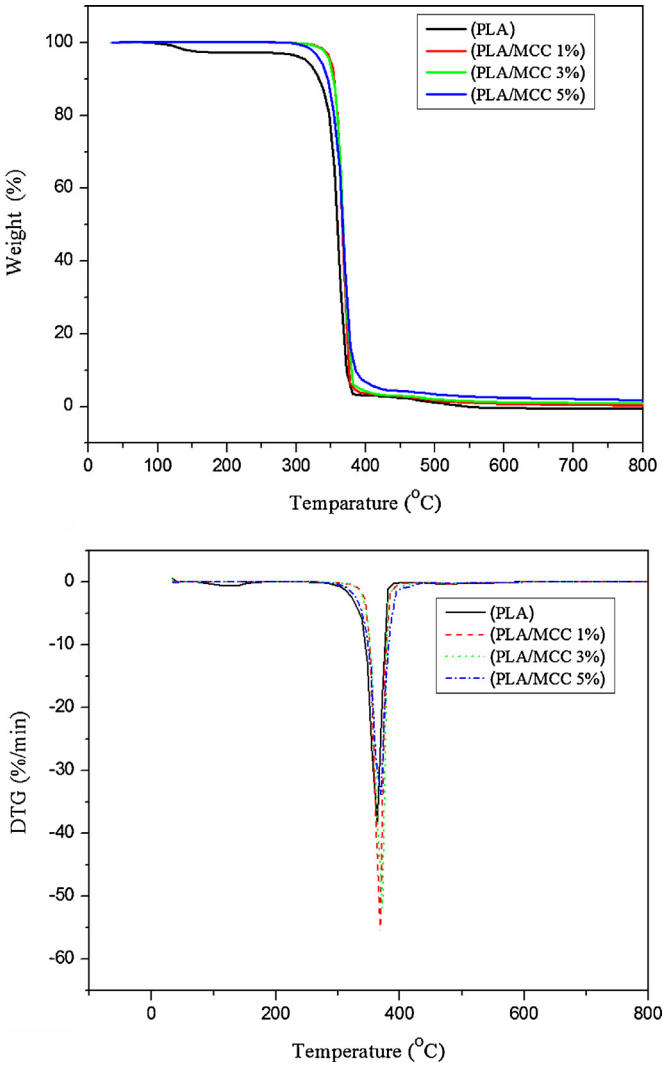

Fig. 2. Typical TGA and DTG curves for pure PLA and PLA/MCC composites.

Table 1
Thermal properties of PLA and PLA/MCC composites.

Samples	Degradation temperature (°C)			Residual weight % at 800 °C
	T_{on}	T_{10}	T_{50}	
PLA	295.93	331.99	359.57	0
PLA/MCC 1%	339.19	354.63	365.95	0.86
PLA/MCC 3%	341.46	352.37	368.21	1.25
PLA/MCC 5%	316.76	343.72	365.95	2.40

at which 10% and 50% weight loss of the samples occurs and the residual weight at 800 °C.

Fig. 2 clearly shows an improvement in thermal stability of the PLA/MCC composites as compared to pure PLA. It can be seen that the onset decomposition temperature (T_{on}), for all PLA/MCC composites were higher than pure PLA (295.93 °C) as well as $T_{10\%}$ and $T_{50\%}$ decomposition temperatures. It is interesting to note that the PLA/MCC 5% composites displayed highest char residue (2.4%) as compared to pure PLA, PLA/MCC 1% and PLA/MCC 3%. This behavior is probably due to the presence of a higher amount of crystalline cellulose I from MCC produced which has an intrinsically flame resistant property (Haafiz, Eichhorn, Hassan, & Jawaid, 2013).

The TGA and DTG curves of neat PLA and PLA/MCC showed a similar decomposition pattern of one-step degradation process represented by a single peak as shown in Fig. 2. The similar result was reported by Zhou, Yu, Zhu, and Qin (2011) when using MCC as reinforcement in poly (3-hydroxybutyrate-co-3-hydroxyvalerate). From Fig. 2, it can be concluded that all PLA/MCC composites produced are thermally more stable than pure PLA. This means that incorporation of the MCC induced the thermal stability of pure PLA. Similar results was also reported by Chuayjuljit, Suuthai, and Charuchinda (2010) when they studied the effect on MCC filled poly (vinyl chloride) film prepared from cotton fabric waste.

3.3. Mechanical properties

The effects of MCC loading on the tensile properties of pure PLA and PLA/MCC composites are shown in Fig. 3. As can be seen in Fig. 3, incorporation of MCC into the PLA matrix did not show any improvements in both tensile strength and elongation at break of the composites as compared to pure PLA. However the Young's modulus was increased from 3.9 GPa to 4.6 GPa with increased MCC loading. The increase in modulus with increasing MCC loading in PLA can be explained by increased in hydrogen bonding, stiffening effect and high crystallinity index of the filler which is a typical characteristics filler/polymer composites (Cheng, Wang, & Rials, 2009). As reported in our previous paper, the relative crystallinity index of MCC obtained was 87% of cellulose I which may have also contributed to the increase in theYoung's modulus of PLA/MCC composites (Kemala, Budianto, & Soegiyono, 2012).

The figure clearly reveals that the tensile strength of the PLA/MCC composites decreased with increasing MCC loading. The low tensile strength for the composites may be attributed to aggregation of the MCC due to Van der Waal's forces (Yew, Mohd Yusof, Mohd Ishak, & Ishiaku, 2005). Due to this phenomenon the filler-filler interaction becomes more pronounced than filler-matrix interaction and there is poor interfacial adhesion between the MCC and the matrix. Therefore the poor adhesion between the matrix and filler generates numerous voids at the filler matrix interface, and the stress transfer to the filler, which is the load bearing entitiy, becomes inefficient leading to low strength values. The result is in agreement with an earlier work reported by Qu, Goa, Wu, and Zhang (2010) and Yew, Mohd Yusof, Mohd Ishak, and Ishiaku (2005).

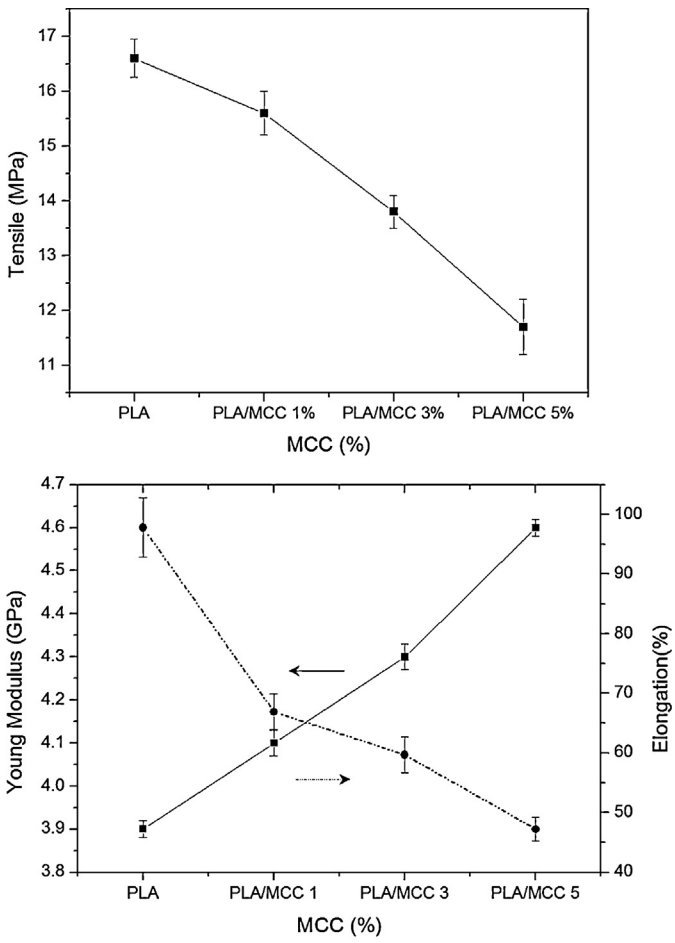

Fig. 3. Typical tensile properties of PLA and PLA/MCC based on MCC (%) loading.

Fig. 3 shows the effect of MCC loading on elongation at break. It can be clearly seen that the elongation at break decreased gradually as the MCC concentration is increased for all PLA/MCC formulations. These observations may be attributed to the stiffening action of the filler by restricting the segmental chain movement of PLA during tensile testing. According to Pei, Qi, and Berglund (2005), the elongation at break is affected by the volume fraction of the added reinforcement, the dispersion of the reinforcement in the matrix, and the interaction between the reinforcement and the matrix. MCC displayed poor interaction and dispersion in PLA matrix due to higher tendency to agglomerate. This cause substantial local stress concentrations and reduced the elongation at break (Cheng, Wang, & Rials, 2009). Further evidence on the dispersion and agglomeration of MCC particles in the PLA matrix is given in SEM analysis, which will be discussed in detail in the next section. From the above results and discussion it can be concluded that, increased MCC contents have a negative effect on PLA/MCC composites strength as compared to the pure PLA due to the agglomeration of MCC particles.

3.4. Microscopy analysis

3.4.1. Scanning electron microscopy (SEM)

SEM of fractured surface of the composites was observed to study the failure mechanisms and to observe the interaction between different components since the mechanical properties depend on polymer/filler interaction (Kemala, Budianto, & Soegiyono, 2012). SEM images of fractured cross-sectional surfaces of PLA and PLA/MCC composites are shown in Fig. 4. The fractured

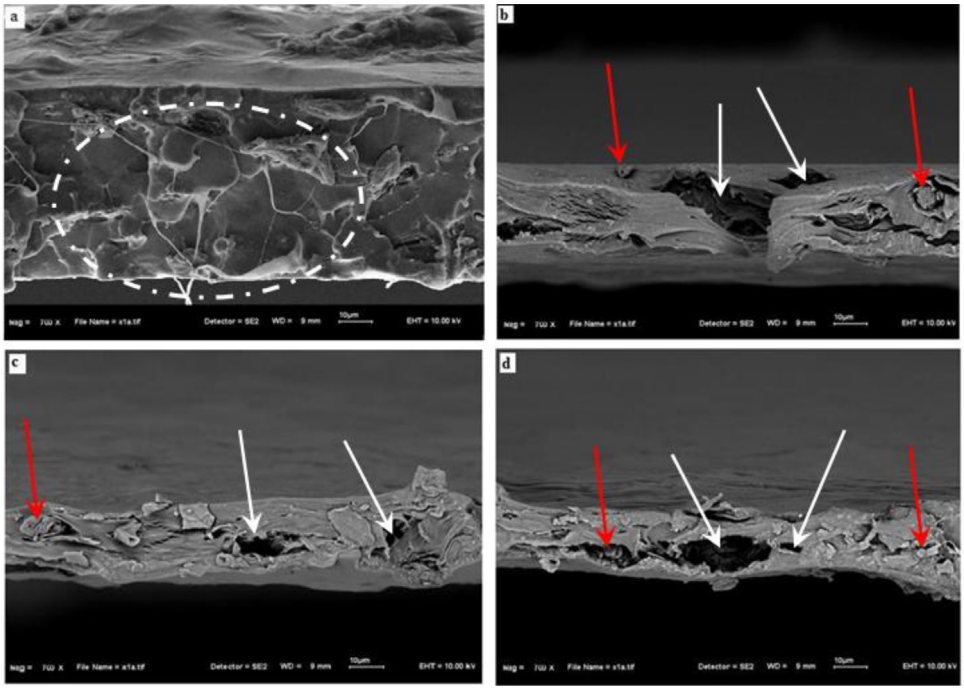

Fig. 4. Typical scanning electron micrographs of fractured cross-sections of (a) PLA, and PLA/MCC with different MCC loading: (b) 1%, (c), 3% and (d) 5% (arrow indicated aggregation (red) and void (white) of MCC). (For interpretation of the references to colour in this figure legend, the reader is referred to the web version of this article.)

surface of pure PLA (Fig. 4a) could be categorized as ductile fracture because the fibrils still remained on the fractured surface. Ductile fractures can be categorized into two groups. Firstly, p high plastic deformation which has fracture-length of remaining fibril of more than 10 μm. Secondly low plastic deformation has fracture-length of remaining fibrils between 1 and 10 μm. The fracture that produce fibrils <1 μm long are categorized as brittle fracture (Yew, Mohd Yusof, Mohd Ishak, & Ishiaku, 2005). The fibril of the PLA in the fractured surface plane is shown as the white circle in Fig. 4a.

After MCC was added in the PLA matrix, the tensile fracture surface of composites showed irregular protrusion and holes (Fig. 4(b)–(d)). This is a typical fractographic feature of a brittle fracture and the agglomerated MCC can be easily seen protruding out of fractured surface. This is a clear indication of poor dispersion of the MCC in PLA matrix. This demonstrated that the dispersion of MCC was not uniform and showed a poor interfacial adhesion between filler and matrix. This may likely be the explanation for the decrease recorded for the tensile strength and elongation at break for PLA/MCC composites as compared to pure PLA. The improvement in Young's modulus is due to the stiffening action of fillers, which is a typical behavior of filled polymer systems. Similar result has been reported by Cheng, Wang, and Rials (2009).

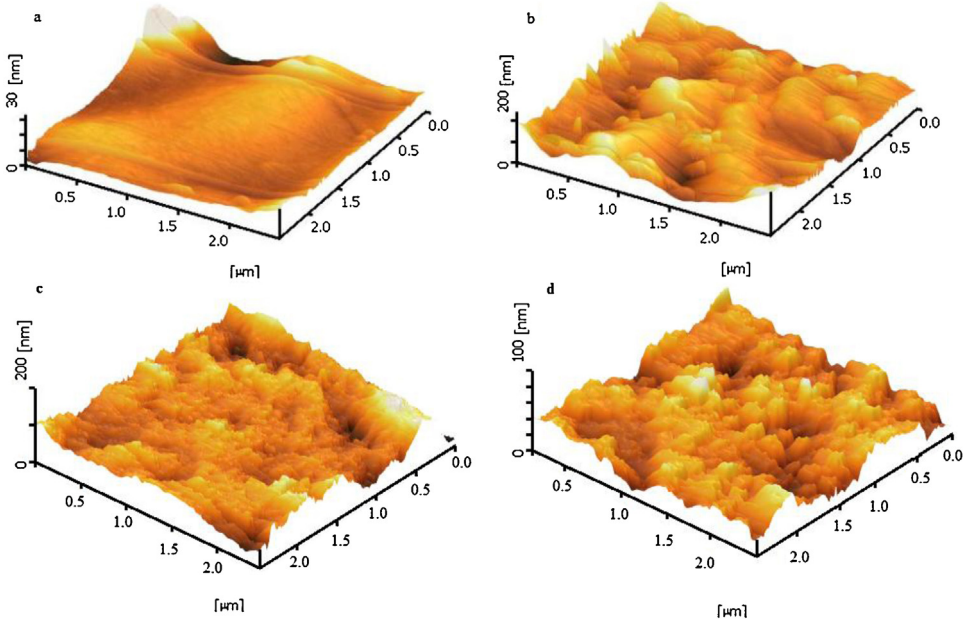

Fig. 5. Typical atomic force microscope images of (a) PLA, and PLA/MCC with different MCC loading: (b) 1%, (c) 3% and (d) 5%.

Fig. 6. Visual comparison of the transparency of (a) PLA and (b) PLA/MCC 1%, (c) PLA/MCC 3% and (d) PLA/MCC 5%.

3.4.2. Atomic force microscopy (AFM)

To further explore the nature of interactions between PLA and PLA/MCC composites, the composites were observed by AFM, and the results are presented in Fig. 5. From the figure, it can be clearly seen that the inclusions of MCC into the PLA matrix significantly change the surface topography of the pure PLA. The pure PLA surface is relatively smooth (Fig. 5(a)). However for PLA/MCC composites (Fig. 5(b)–(d)) the cluster between PLA and MCC are readily apparent and the surface cluster a clearly observed when the MCC contents are increased. The cluster features are interpreted as the result of aggregation of the MCC, or as PLA coated MCC. Similar result was earlier reported by Saxena, Elder, Pan, and Ragauskas (2009).

3.5. Film transparency

The visual study of the transparency of PLA and the PLA/MCC composites with different MCC contents are presented in Fig. 6. Generally, the transparency of the PLA/MCC composites was good but as seen in Fig. 6(b)–(d) some white spots are visible in the PLA/MCC composites and were clearly observed as the MCC content was increased. These spots are expected to be MCC aggregates in the PLA matrix. The synthesized PLA/MCC composites is characterized by good thermal properties and can be used in packaging, automotive and medical applications where properties such strength and stiffness are not important.

4. Conclusion

PLA/MCC composites were successfully fabricated by solution casting technique. The FT-IR spectra of PLA/MCC revealed no significant changes in the peak positions suggesting that only physical interaction between PLA and MCC occurred. TGA results indicated that the PLA/MCC composites displayed better thermal stability as compared to that pure PLA. Tensile properties of the cast composites showed an increase in Young's modulus with increasing MCC content due the stiffening action of MCC. However, both tensile strength and elongation at break decreased with increasing MCC content due to poor dispersion of MCC in PLA matrix and subsequent chain restriction movement respectively. The morphological observations using SEM and AFM showed the poor dispersion of MCC in the composites, which could account for the decrease in tensile properties of PLA/MCC composites. The present challenges are to find an effective method to disperse MCC in PLA and to improve adhesion between the filler and polymer. This is expected to enhance the composite's tensile properties.

Acknowledgements

The author M.K. Mohamad Haafiz would like to thank University Sains Malaysia (USM), Ministry of Higher Education Malaysia (KPT) and Research University Grant 05H22 sub-code Q.J130000.2509.05H22 for financial support.

References

Battista, O. A. (1950). Hydrolysis and crystallization of cellulose. *Industrial and Engineering Chemistry*, *42*, 502–507.
Bondeson, D., Mathew, A., & Oksman, K. (2006). Optimization of the isolation of nanocrystals from microcrystalline cellulose by acid hydrolysis. *Cellulose*, *13*, 171–180.
Cheng, Q., Wang, S., & Rials, T. G. (2009). Poly (vinyl alcohol) nanocomposites reinforced with cellulose fibrils isolated by high intensity ultrasonication. *Composites Part A Applied Science and Manufacturing*, *40*, 218–224.
Chuayjuljit, S., Su-uthai, S., & Charuchinda, S. (2010). Poly(vinyl chloride) film filled with microcrystalline cellulose prepared from cotton fabric waste: properties and biodegradability study. *Waste Management & Research*, *28*, 109–117.
Eichhorn, S. J., Dufresne, A., Aranguren, M., Marcovich, N. E., Capadona, J. R., Rowan, S. J., et al. (2010). Review: current international research into cellulose nanofibres and nanocomposites. *Journal of Material Science*, *45*, 1–33.
El-Sakhawy, M., & Hassan, M. L. (2007). Physical and mechanical properties of microcrystalline cellulose prepared from agricultural residues. *Carbohydrate Polymer*, *67*, 1–10.
Haafiz, M. K. M., Eichhorn, S. J., Hassan, A., & Jawaid, M. (2013). Isolation and characterization of microcrystalline cellulose from oil palm biomass residue. *Carbohydrate polymer*, *93*, 628–634.
Jonoobi, M., Harun, J., Mathew, A. P., & Oksman, K. (2010). Mechanical properties of cellulose nanofiber (CNF) reinforced polylactic acid (PLA) prepared by twin screw extrusion. *Composites Science and Technology*, *97*.
Kemala, T., Budianto, E., & Soegiyono, B. (2012). Preparation and characterization of microspheres based on blend of poly (lactic acid) and poly (ε-caprolactone) with poly (vinyl alcohol) as emulsifier. *Arabian Journal of Chemistry*, *5*, 103–108.
Kumar, V., Maria De La, L. R. M., & Yang, D. (2002). Preparation, characterization and tabletting properties of a new cellulose-based pharmaceutical aid. *International Journal of Pharmaceutics*, *235*, 129–140.
Maria, D., Garcia, S., & Lagaron, J. M. (2010). On the use of plant cellulose nanowhiskers to enhance the barrier properties of polylactic acid. *Cellulose*, *17*.
Mathew, A. P., Oksman, K., & Sain, M. (2005). Mechanical properties of biodegradable composites from poly lactic acid (PLA) and microcrystalline cellulose (MCC). *Journal of Applied Polymer Science.*, *97*, 2014–2025.
Nakagaito, A. N., Fujimura, A., Sakai, T., Hama, Y., & Yano, H. (2009). Production of microfibrillated cellulose (MFC)-reinforced polylactic acid (PLA) nanocomposites from sheets obtained by a papermaking-like process. *Composites Science and Technology*, *69*, 1293–1297.
Oksman, K., Mathew, A. P., Bondeson, D., & Kvien, I. (2006). Manufacturing process of cellulose whiskers/polylactic acid nanocomposites. *Composites Science and Technology*, *66*, 2776–2784.
Pamula, E., Blazeeicz, M., Paluszkiewiez, C., & Dobrzyński. (2001). FTIR study of degradation products of aliphatic polyester–carbon fibres composites. *Journal of Molecular Structure*, *596*, 69–75.
Pei, A., Qi, Z., & Berglund, L. A. (2005). Functionalized cellulose nanocrystals as biobased nucleation agents in poly (L-lactide) (PLLA) – crystallization and mechanical property effects. *Composites Science and Technology*, *70*, 815–821.
Petersson, L., Kvien, I., & Oksman, K. (2007). Structure and thermal properties of poly (lactic acid)/cellulose whiskers nanocomposite materials. *Composites Science and Technology*, *67*, 2535–2544.
Petersson, L., & Oksman, K. (2006). Biopolymer based nanocomposites: comparing layered silicates and microcrystalline cellulose as nanoreinforcement. *Composites Science and Technology*, *66*, 2187–2196.
Pullawan, T., Wilkinson, A. N., & Eichhorn, S. J. (2010). Discrimination of matrix–fibre interactions in all-cellulose nanocomposites. *Composites Science and Technology*, *70*, 2325–2330.
Qu, P., Goa, Y., Wu, G. F., & Zhang, L. P. (2010). Nanocomposite of poly (lactic acid) reinforced with cellulose nanofibrils. *BioResources*, *5*(3), 1811–1823.
Rånby, B. G. (1951). *Cellulose and muscle – The colloidal properties of cellulose micelles*. Discussions of the Faraday Society, 11, 158–164, Discussion.
Samir, M. A. S. A., Alloin, F., & Dufresne, A. (2005). Review of recent research into cellulosic whiskers, their properties and their application in nanocomposite field. *Biomacromolecules*, *6*, 612–626.
Saxena, A., Elder, T. J., Pan, S., & Ragauskas, A. J. (2009). Novel nanocellulosic xylan composite film. *Composites Part B Engineering*, *40*, 727–730.

Siqueira, G., Bras, J., & Dufresne, A. (2009). Cellulose whiskers versus microfibrils: influence of the nature of the nanoparticle and its surface functionalization on the thermal and mechanical properties of nanocomposites. *Biomacromolecules*, *10*, 425–432.

Sturcova, A., Davies, G. R., & Eichhorn, S. J. (2005). Elastic modulus and stress-transfer properties of tunicate cellulose whiskers. *Biomacromolecules*, *6*, 1055–1061.

Suryanegara, L., Nakagaito, A. N., & Yano, H. (2009). The effect of crystallization of PLA on the thermal and mechanical properties of microfibrillated cellulose-reinforced PLA composites. *Composites Science and Technology*, *69*.

Yew, G. H., Mohd Yusof, A. M., Mohd Ishak, Z. A., & Ishiaku, U. S. (2005). Water absorption and enzymatic degradation of poly (lactic acid)/rice starch composites. *Polymer Degradation and Stability*, *90*, 488–500.

Zhou, Z., Yu, H., Zhu, M., & Qin, Z. (2011). Effects of microcrystalline cellulose on the thermal properties of poly (3-hydroxybutyrate-co-3 hydroxyvalerate). *Advanced Materials Research*, *284*(286), 1778–1781.